--- SUPPLEMENTARY INFORMATION ---

Histone deacetylase 6 structure and molecular basis of catalysis and inhibition

Yang Hai[1] & David W. Christianson[1,2]*

[1]Roy and Diana Vagelos Laboratories, Department of Chemistry, University of Pennsylvania, Philadelphia, Pennsylvania 19104-6323, USA. [2]Radcliffe Institute for Advanced Study and Department of Chemistry and Chemical Biology, Harvard University, Cambridge, Massachusetts 02138, USA. *e-mail: chris@sas.upenn.edu

SUPPLEMENTARY RESULTS

Supplementary Table 1. Steady-state kinetics of HDAC6 catalytic domains[a]

Substrate 1	**K_M (μM)**	**k_{cat} (s^{-1})**	**k_{cat}/K_M ($M^{-1}s^{-1}$)**
hCD12	22 ± 6	0.05 ± 0.01	(2.3 ± 0.9) x 10^3
hCD12 Y386F	26 ± 9	0.06 ± 0.02	(2.3 ± 0.9) x 10^3
hCD12 Y782F	62 ± 4	0.00030 ± 0.00002	4.8 ± 0.3
hCD12 Y386F/Y782F	69 ± 3	0.00021 ± 0.00001	3.0 ± 0.2
zCD12	38 ± 6	0.8 ± 0.1	(2.10 ± 0.08) x 10^4
zCD12 H194A	31 ± 9	0.7 ± 0.1	(2.3 ± 0.8) x 10^4
zCD12 H574A	65 ± 9	0.082 ± 0.007	(1.2 ± 0.1) x 10^3
zCD1	87 ± 9	0.079 ± 0.006	(0.9 ± 0.1) x 10^3
zCD2	29 ± 9	0.56 ± 0.09	(1.9 ± 0.5) x 10^4
Substrate 8	**K_M (μM)**	**k_{cat} (s^{-1})**	**k_{cat}/K_M ($M^{-1}s^{-1}$)**
hFLWT[b]	7 ± 4	0.04 ± 0.01	(6 ± 1) x 10^3
hCD12	11 ± 4	0.049 ± 0.009	(4.4 ± 0.9) x 10^3
hCD1	n.a.	n.a.	n.a.
hCD2	22 ± 3	0.020 ± 0.002	(0.91 ± 0.03) x 10^3
hCD12 Y386F	16 ± 4	0.06 ± 0.02	(4 ± 1) x 10^3
hCD12 Y782F	42 ± 4	0.0003 ± 0.0001	7 ± 2
hCD12 Y386F/Y782F	39 ± 3	0.0004 ± 0.0002	9 ± 2
hCD12 Y225F/Y782F	56 ± 9	0.048 ± 0.004	(0.86 ± 0.06) x 10^3
hCD12 K353L/Y782F	52 ± 6	0.002 ± 0.001	40 ± 10
hCD2 D567A	26 ± 3	0.022 ± 0.006	(0.8 ± 0.1) x 10^3
hCD2 S568A	21 ± 5	0.0020 ± 0.0007	90 ± 10
zCD12	28 ± 3	0.98 ± 0.09	(3.5 ± 0.5) x 10^4
zCD12 H194A	19 ± 6	0.60 ± 0.05	(3.2 ± 0.4) x 10^4
zCD12 H574A	38 ± 7	0.23 ± 0.07	(6.2 ± 0.9) x 10^3
zCD1	43 ± 6	0.20 ± 0.06	(4.7 ± 0.3) x 10^3
zCD1 K330L	32 ± 7	0.155 ± 0.009	(5 ± 1) x 10^3
zCD1 H82F/F202Y	47 ± 4	0.016 ± 0.006	(0.34 ± 0.9) x 10^3
zCD2	22 ± 9	0.69 ± 0.08	(3.1 ± 0.5) x 10^4
zCD2 H573A	8 ± 3	0.00021 ± 0.00004	26 ± 4
zCD2 H574A	9 ± 2	0.0006 ± 0.0001	67 ± 6
zCD2 N530A	40 ± 10	0.7 ± 0.1	(1.7 ± 0.9) x 10^4
zCD2 S531A	240 ± 40	0.03 ± 0.01	(0.12 ± 0.04) x 10^3

Substrate 9	**K_M (µM)**	**k_{cat} (s^{-1})**	**k_{cat}/K_M ($M^{-1}s^{-1}$)**
hCD12	100 ± 20	0.26 ± 0.02	(2.7 ± 0.5) x 10^3
hCD12 Y386F	90 ± 40	0.18 ± 0.04	(1.9 ± 0.9) x 10^3
hCD12 Y782F	50 ± 10	0.080 ± 0.006	(1.5 ± 0.4) x 10^3
zCD1	100 ± 20	0.9 ± 0.1	(8.6 ± 0.9) x 10^3
zCD2	140 ± 50	1.2 ± 0.3	(8.0 ± 2.0) x 10^3
zCD12	110 ± 30	2.0 ± 0.3	(1.9 ± 0.4) x 10^4
Substrate 10	**K_M (µM)**	**k_{cat} (s^{-1})**	**k_{cat}/K_M ($M^{-1}s^{-1}$)**
hCD12	80 ± 20	0.20 ± 0.02	(2.3 ± 0.4) x 10^3
hCD12 Y386F	120 ± 20	0.13 ± 0.01	(2.3 ± 0.4) x 10^3
hCD12 Y782F	80 ± 10	0.078 ± 0.005	(1.0 ± 0.1) x 10^3
zCD1	120 ± 40	0.9 ± 0.2	(7.0 ± 2.0) x 10^3
zCD2	110 ± 20	0.82 ± 0.08	(7.3 ± 0.7) x 10^3
zCD12	80 ± 20	1.5 ± 0.1	(1.9 ± 0.2) x 10^4
Substrate 11	**K_M (µM)**	**k_{cat} (s^{-1})**	**k_{cat}/K_M ($M^{-1}s^{-1}$)**
hCD12	210 ± 70	0.11 ± 0.04	(0.59 ± 0.08) x 10^3
hCD12 Y386F	140 ± 60	0.10 ± 0.02	(0.7 ± 0.2) x 10^3
hCD12 Y782F	n.a.	n.a.	n.a.
zCD1	n.d.[d]	n.d.	11 ± 6
zCD2	110 ± 20	0.44 ± 0.04	(4.0 ± 0.4) x 10^3
zCD12	150 ± 30	0.62 ± 0.08	(4.2 ± 0.5) x 10^3
Substrate 12	**K_M (µM)**	**k_{cat} (s^{-1})**	**k_{cat}/K_M ($M^{-1}s^{-1}$)**
hCD12	70 ± 30	0.25 ± 0.04	(4 ± 1) x 10^3
hCD12 Y386F	80 ± 30	0.26 ± 0.04	(3.1 ± 0.9) x 10^3
hCD12 Y782F	n.a.	n.a.	n.a.
zCD1	90 ± 30	0.047 ± 0.006	(0.6 ± 0.1) x 10^3
zCD2	80 ± 20	0.9 ± 0.1	(1.2 ± 0.2) x 10^4
zCD12	70 ± 10	1.3 ± 0.1	(1.8 ± 0.3) x 10^4
Substrate 13	**K_M (µM)**	**k_{cat} (s^{-1})**	**k_{cat}/K_M ($M^{-1}s^{-1}$)**
hCD12	70 ± 20	0.07 ± 0.01	(0.9 ± 0.1) x 10^3
hCD12 Y386F	60 ± 7	0.060 ± 0.002	(0.97 ± 0.08) x 10^3
hCD12 Y782F	n.d.	n.d.	3 ± 1
zCD1	n.d.	n.d.	20 ± 10
zCD2	130 ± 50	0.39 ± 0.07	(3.0 ± 0.7) x 10^3
zCD12	200 ± 40	0.58 ± 0.06	(2.9 ± 0.4) x 10^3

[a]Data represent mean values ± s.e.m. (n=3). [b]hFLWT, human full-length wild-type HDAC6 from Enzo Life Sciences. [c]n.a., no activity. [d]n.d., not determined.

Supplementary Table 2. Data collection and refinement statistics.

	zCD1-TSA complex	zCD2-TSA complex	MBP-hCD2-TSA complex	Unliganded zCD2
Data collection				
Space group	$P2_1$	$P2_12_12$	$P2_12_12_1$	$P1$
Cell dimensions				
a, b, c (Å),	52.9, 123.7, 55.2	83.9, 94.4, 51.7	49.3, 149.0, 216.3	48.5, 55.4, 74.2
α, β, γ (°)	90.0, 113.8, 90.0	90.0, 90.0, 90.0	90.0, 90.0, 90.0	73.6, 89.8, 82.6
Resolution (Å)*	45.04 - 2.15	50.00 - 1.59	149.00 - 2.79	50.00 - 2.00
	(2.24 - 2.15)	(1.66 - 1.59)	(2.90 - 2.79)	(2.08 - 2.00)
R_{merge}	0.178 (0.701)	0.061 (0.033)	0.204 (1.853)	0.162 (0.501)
R_{pim}	0.122 (0.493)	0.050 (0.297)	0.141 (0.607)	0.162 (0.509)
I / σI	10.6 (2.0)	23.7 (4.3)	12.9 (1.9)	6.4 (1.8)
Completeness (%)	99.0 (95.9)	100.0 (100.0)	100.0 (100.0)	97.0 (96.6)
Redundancy[a]	3.1 (2.8)	2.5 (2.4)	11.0 (11.3)	1.9 (1.9)
$CC_{1/2}$	0.754 (0.536)	0.935 (0.865)	0.986 (0.585)	0.967 (0.662)
Refinement				
Resolution (Å)	45.04 - 2.15	44.01 - 1.59	87.54 - 2.79	15.91 - 2.00
	(2.23 - 2.15)	(1.65 - 1.59)	(2.89 - 2.79)	(2.07 - 2.00)
No. reflections	34834 (3335)	55924 (5519)	40788 (4012)	47957 (4586)
R_{work} / R_{free}	0.211/0.255	0.129/0.163	0.213/0.275	0.224/0.272
	(0.282/0.325)	(0.128/0.187)	(0.313/0.377)	(0.276/0.316)
No. atoms				
Protein	5558	2836	3260	5541
Ligand/ion	63	77	77	12
Water	164	376	355	305
B factors (Å^2)				
Protein	32	13	55	17
Ligand/ion	34	32	62	25
Water	30	28	59	21
R.m.s. deviations				
bond lengths (Å)	0.006	0.010	0.004	0.006
bond angles (°)	0.9	1.2	0.8	1.0

Each dataset was collected from a single crystal. *Values in parentheses are for highest-resolution shell.

Supplementary Table 3. Data collection and refinement statistics.

	H574A zCD2-substrate **8** complex	Y785F zCD2-substrate **1** complex	zCD2-HC toxin complex	zCD2-trifluoro-ketone inhibitor complex	zCD2-acetate complex
Data collection					
Space group	$P2_1$	$P2_12_12$	$P2_12_12$	$P2_12_12_1$	$P2_12_12_1$
Cell dimensions					
a, b, c (Å),	55.0, 84.0, 87.0	83.3, 94.7,51.6	83.5, 94.1, 51.5	74.6, 92.4, 96.2	75.1, 91.8, 96.2
α, β, γ (^{o})	90.0, 98.1, 90.0	90.0, 90.0 90.0	90.0, 90.0, 90.0	90.0, 90.0, 90.0	90.0, 90.0, 90.0
Resolution (Å)*	50.00 - 1.80	50.00 - 1.82	50.00 - 1.73	50.00 - 2.16	50.00 - 2.25
	(1.87 - 1.80)	(1.88 - 1.82)	(1.79 - 1.73)	(2.24 - 2.16)	(2.33 - 2.25)
R_{merge}	0.142 (0.713)	0.164 (0.655)	0.151 (0.442)	0.148 (0.334)	0.130 (0.356)
R_{pim}	0.098 (0.509)	0.049 (0.344)	0.061 (0.273)	0.061 (0.178)	0.055 (0.212)
I / σI	9.9 (1.8)	13.6 (1.1)	14.0 (1.6)	13.5 (3.0)	14.5 (2.8)
Completeness (%)	98.9 (99.9)	99.4 (94.1)	98.7 (90.6)	98.8 (90.3)	99.3 (93.9)
Redundancy[a]	3.0 (3.0)	11.0 (4.1)	6.6 (3.1)	6.6 (3.9)	6.3 (3.5)
$CC_{1/2}$	0.975 (0.524)	0.958 (0.692)	0.976 (0.808)	0.977 (0.933)	0.969 (0.856)
Refinement					
Resolution (Å)	12.34 - 1.80	45.32 - 1.81	47.07 - 1.73	49.71 - 2.16	49.77 - 2.24
	(1.87 - 1.80)	(1.88 - 1.81)	(1.79 - 1.73)	(2.24 - 2.16)	(2.33 - 2.24)
No. reflections	70922 (6942)	37343 (3333)	42831 (3774)	35829 (3223)	32149 (2879)
R_{work} / R_{free}	0.162/0.194	0.157/0.183	0.152/0.173	0.196/0.242	0.212/0.234
	(0.238/0.270)	(0.260/0.265)	(0.224/0.244)	(0.221/0.275)	(0.280/0.319)
No. atoms					
Protein	5718	2792	2817	5581	5603
Ligand/ion	28	33	25	24	22
Water	25	29	27	23	26
B factors (Å^2)					
Protein	5718	2792	2817	5581	5603
Ligand/ion	28	33	25	24	22
Water	25	29	27	23	26
R.m.s. deviations					
bond lengths (Å)	0.008	0.009	0.012	0.005	0.005
bond angles (^{o})	1.0	1.1	1.2	1.0	1.0

Each dataset was collected from a single crystal. *Values in parentheses are for highest-resolution shell.

Supplementary Table 4. Data collection and refinement statistics.

	zCD2-SAHA complex	zCD2-Belinostat complex	zCD2-HPOB complex	zCD2-Panobinostat complex	zCD2-Oxamflatin complex
Data collection					
Space group	$P2_1$	$P2_12_12_1$	$P1$	$P2_12_12$	$P2_12_12$
Cell dimensions					
a, b, c (Å),	54.8, 83.6, 86.8	76.0, 95.5, 96.3	48.7, 56.6, 74.8	65.2, 91.9, 140.4	83.5, 94.4, 51.6
α, β, γ (^{o})	90.0, 98.1, 90.0	90.0, 90.0, 90.0	106.4, 90.1, 97.1	90.0, 90.0, 90.0	90.0, 90.0, 90.0
Resolution (Å)*	50.00 - 1.32	50.00 - 1.85	50.60 - 1.90	50.00 - 2.60	50.00 - 2.54
	(1.38 - 1.32)	(1.92 - 1.85)	(1.97 - 1.90)	(2.71 - 2.60)	(2.63 - 2.54)
R_{merge}	0.124 (1.170)	0.167 (0.831)	0.143 (0.754)	0.217 (0.699)	0.137 (0.311)
R_{pim}	0.043 (0.481)	0.078 (0.328)	0.114 (0.640)	0.088 (0.334)	0.065 (0.185)
I / σI	40.0 (2.0)	13.0 (1.6)	6.9 (1.6)	8.3 (1.6)	11.6 (3.1)
Completeness (%)	95.0 (90.7)	99.7 (100)	97.5 (95.7)	99.4 (95.6)	98.8 (92.1)
Redundancy[a]	3.3 (3.1)	7.5 (7.4)	3.2 (3.2)	6.9 (4.8)	4.9 (3.1)
$CC_{1/2}$	0.706 (0.215)	0.996 (0.895)	0.982 (0.480)	0.984 (0.703)	0.974 (0.882)
Refinement					
Resolution (Å)	36.26 - 1.32	17.06 - 1.86	50.55 - 1.90	49.71 - 2.60	47.22 - 2.54
	(1.37 - 1.32)	(1.92 - 1.86)	(1.97 - 1.90)	(2.69 - 2.60)	(2.63 - 2.54)
No. reflections	170694 (15998)	(59011/5804)	58345 (5700)	26488 (2368)	13596 (1131)
R_{work} / R_{free}	0.125/0.147	0.183/0.224	0.181/0.288	0.189/0.265	0.147/0.157
	(0.241/0.273)	(0.267/0.314)	(0.221/0.356)	(0.234/0.325)	(0.194/0.214)
No. atoms					
Protein	5733	5570	5572	5595	2778
Ligand/ion	83	52	52	80	27
Water	644	343	442	205	143
B factors (Å^2)					
Protein	18	22	18	26	17
Ligand/ion	28	27	36	38	26
Water	30	28	27	26	20
R.m.s. deviations					
bond lengths (Å)	0.010	0.006	0.009	0.005	0.009
bond angles (^{o})	1.2	0.9	1.1	0.9	1.1

Each dataset was collected from a single crystal. *Values in parentheses are for highest-resolution shell.

Supplementary Table 5. Hydroxamate inhibitor-Zn^{2+} coordination interactions.

	HO---Zn^{2+} distance (Å)	C=O---Zn^{2+} distance (Å)
hCD2-TSA	2.0	2.3
	2.2	2.6
zCD1-TSA	1.9	2.9
	2.0	2.5
zCD2-TSA	2.2	2.4
zCD2-SAHA	2.1	2.2
	2.0	2.2
zCD2-Panobinostat	2.0	2.6
	2.1	3.5
zCD2-Belinostat	2.2	2.4
	2.1	2.6
zCD2-Oxamflatin	2.2	2.3

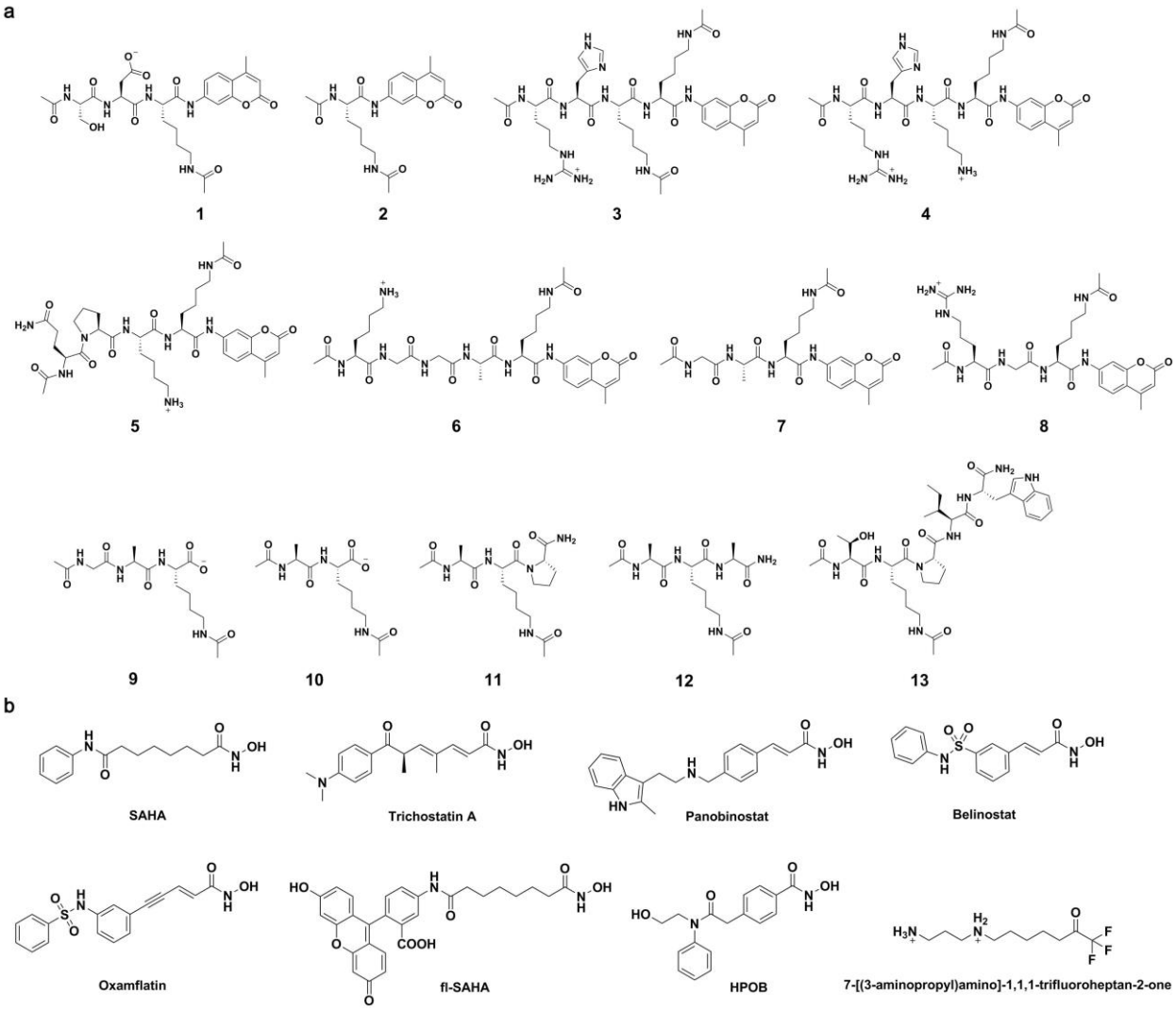

Supplementary Figure 1. HDAC6 substrates 1-13 and inhibitors. (a) Peptide substrates used for HDAC6 activity assays (AMC = aminomethylcoumarin). These commercially available substrates were selected based on their peptide sequence variations, which allowed us to probe HDAC6 substrate specificity. **1**, Ac-Ser-Asp-Lys(Ac)-AMC, derived from α-tubulin. **2**, Ac-Lys(Ac)-AMC, generic acetyllysine substrate. **3**, Ac-Arg-His-Lys(Ac)-Lys(Ac)-AMC, derived from p53. **4**, Arg-His-Lys-Lys(Ac)-AMC, derived from p53. **5**, Ac-Gln-Pro-Lys-Lys(Ac)-AMC, derived from p53. **6**, Ac-Lys-Gly-Gly-Ala-Lys(Ac)-AMC, derived from histone H4. **7**, Ac-Gly-Ala-Lys(Ac)-AMC, derived from histone H4. **8**, Ac-Arg-Gly-Lys(Ac)-AMC, derived from histone H4. **9**, Ac-Gly-Ala-Lys(Ac), derived from histone H4. **10**, Ac-Ala-Lys(Ac), derived from histone H4. **11**, Ac-Ala-Lys(Ac)-Pro-NH_2, artificial acetyllysine substrate. **12**, Ac-Ala-Lys(Ac)-Ala-NH_2, artificial acetyllysine substrate. **13**, Ac-Thr-Lys(Ac)-Pro-Ile-Trp-NH_2, derived from Hsp90. **(b)** Inhibitors used in this study. Abbreviations: SAHA, suberanilohydroxamic acid; fl-SAHA, fluorescein-SAHA; HPOB, *N*-hydroxy-4-(2-[(2-hydroxyethyl)(phenyl)amino]-2-oxoethyl)benzamide.

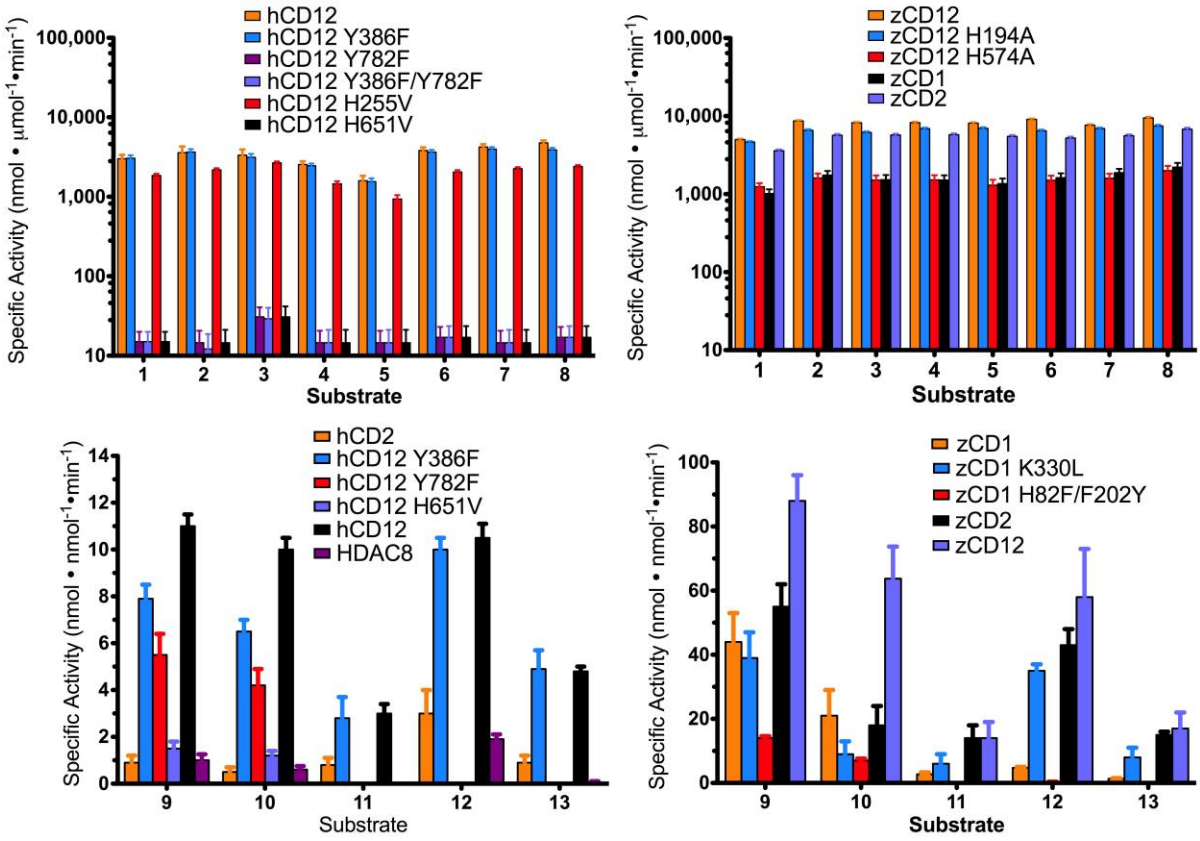

Supplementary Figure 2. Enzyme activity measurements. Specific activities of human and zebrafish HDAC6 constructs assayed with fluorogenic substrates **1**–**8** and nonfluorogenic substrates **9**–**13** (substrates are illustrated in **Supplementary Fig. 1a**; data represent mean values ± s.d. (n=3)). No activity is observed with hCD1 and Y386F/Y782F hCD12, so these constructs do not appear in the figure.

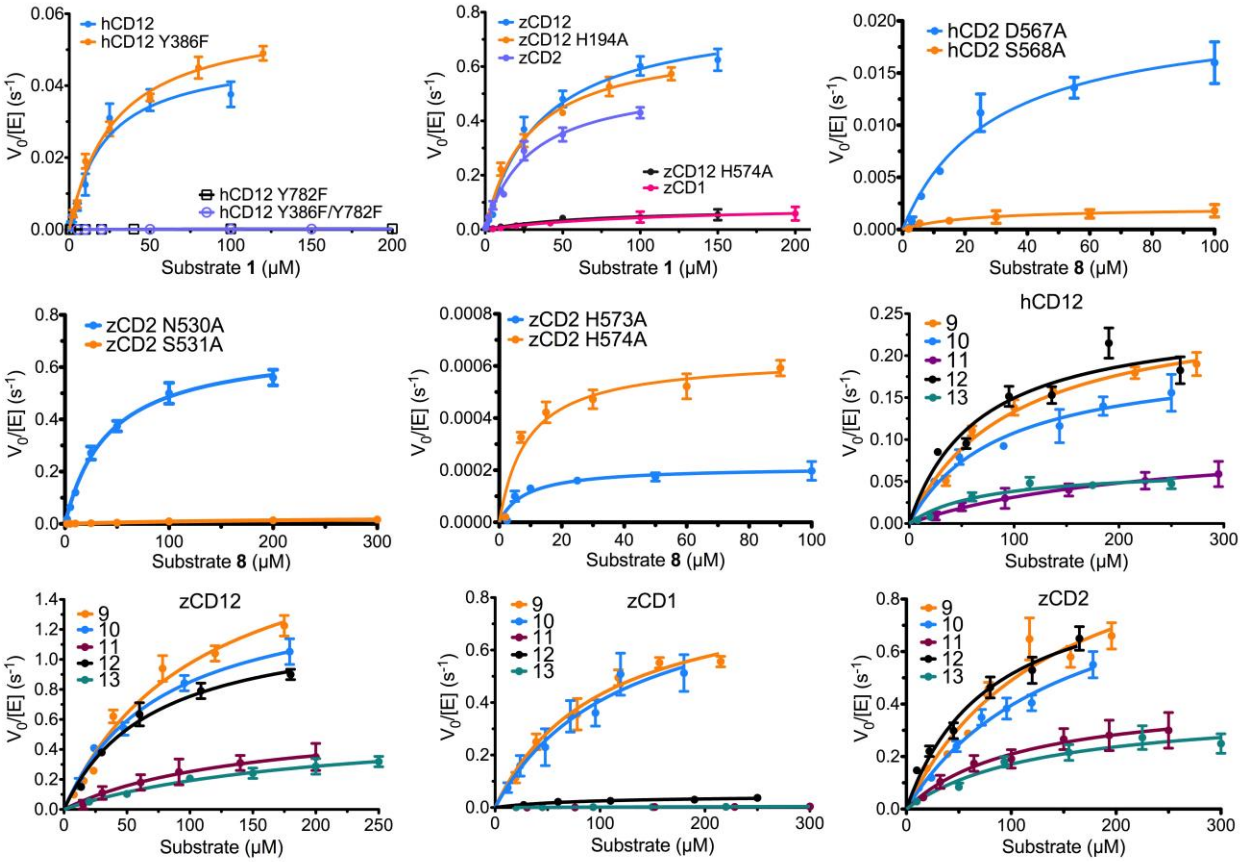

Supplementary Figure 3. Michaelis-Menten plots. Steady-state kinetics for human and zebrafish HDAC6 constructs assayed with fluorogenic substrates **1**–**8** and nonfluorogenic substrates **9**–**13** (substrates are illustrated in **Supplementary Fig. 1a**; data represent mean values ± s.d. (n=3)).

a

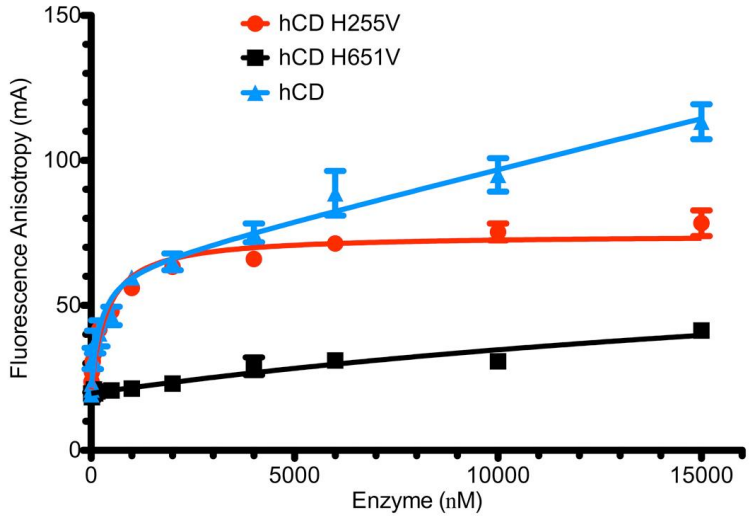

b

Binding affinity of fl-SAHA determined by fluorescence anisotropy.[a]

Enzymes	K_d (μM)
hCD12	K_{d1} = 0.2 ± 0.1, K_{d2} > 40[b]
hCD12 H255V	0.24 ± 0.09
hCD12 H651V	30 ± 20
zCD1	1.6 ± 0.3
zCD1 H82F/F202Y	2.9 ± 0.7
zCD2	0.05 ± 0.02
zCD2 S531A	0.17 ± 0.04

[a] Similar affinity trends are observed for inhibitor binding to the catalytic domains of human and zebrafish HDAC6, in that the fluorescent inhibitor binds to CD1 domains with lower affinity than to CD2 domains. While inhibitor affinity is lower for zCD1 compared with zCD2, it is not as low as that for hCD1 compared with hCD2. [b] K_{d2} cannot be accurately determined due to nonsaturating data.

Supplementary Figure 4. Ligand binding to catalytic domains of hHDAC6. (a) We probed inhibitor binding to hHDAC6 using fluorescence anisotropy spectroscopy and fl-SAHA (**Supplementary Fig. 1b**). Ligand binding is characterized by a biphasic curve indicating a high affinity site (K_{d1} = 0.2 ± 0.1 μM) and a low affinity site (K_d > 40 μM) (data represent mean (n=3) ± s.d.). We then disabled ligand binding in each domain by mutating Zn^{2+} ligand H255V in hCD1 and H651V in hCD2. H255V hCD12 retains high affinity ligand binding activity, whereas H651V hCD12 exhibits 150-fold diminished affinity. These results are consistent with high-affinity binding only to hCD2. **(b)** Binding affinities of fl-SAHA to human and zebrafish HDAC6 constructs (data represent mean ± s.e.m. (n=3)).

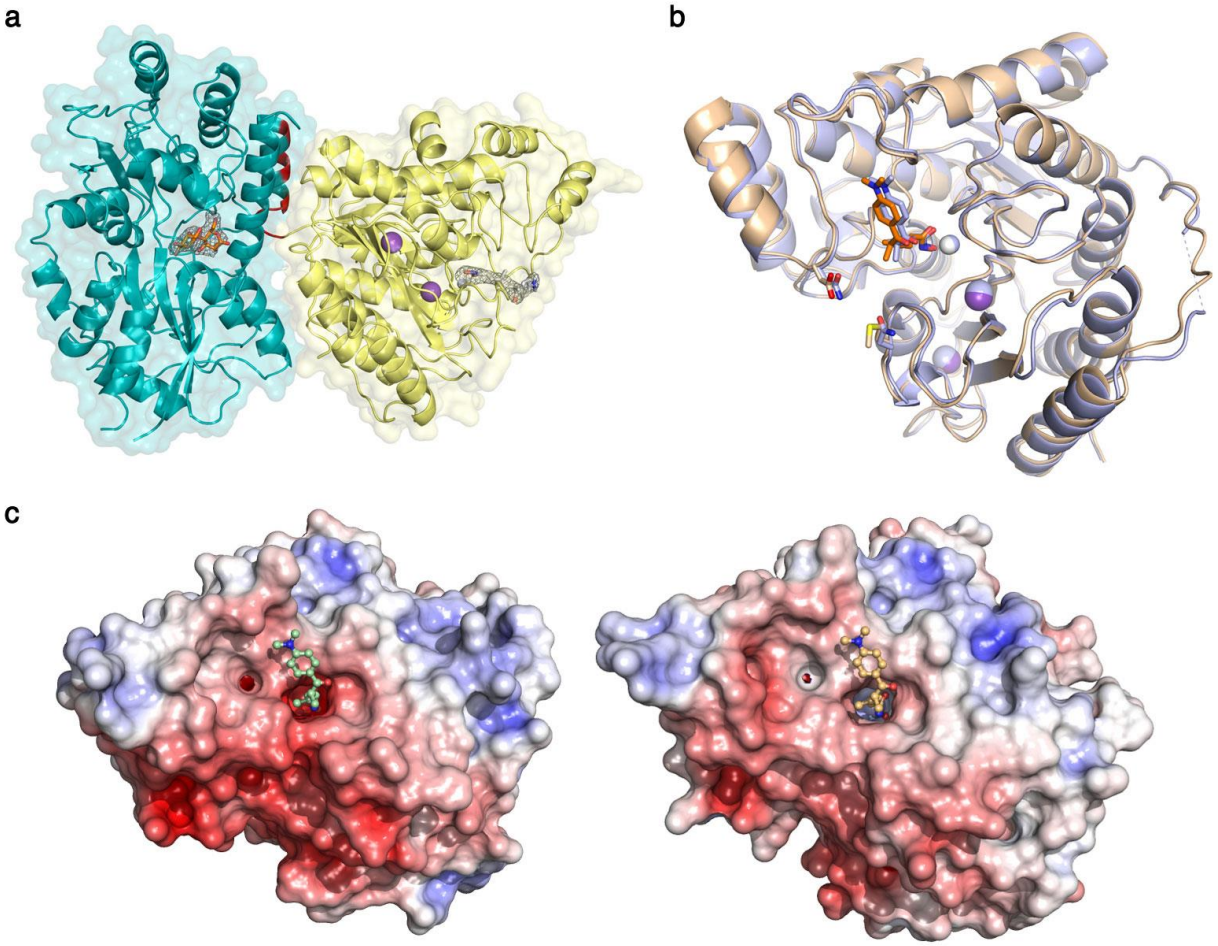

Supplementary Figure 5. Crystal structure of MBP-hCD2 complexed with maltose and TSA. (a) Simulated annealing omit map (grey mesh, 3.0σ) shows ligands bound to each protein. The linker (red) consists of the C-terminus of MBP (containing mutations D358A, E359A, K362A, D363A, R367N, and ΔI368-K370) linked to an Ala_3 segment, which then connects to the N-terminus of hCD2. This engineered linker forms an α-helix (red) that provides a complementary surface that facilitates MBP-hCD2 interactions. **(b)** Superposition of the hCD2-TSA (wheat; orange TSA) and zCD2-TSA (light blue; blue TSA) complexes. Residues D770-H771 in zCD2 are disordered and indicated by a dotted line on the right-hand side of the image. The Zn^{2+} ion and K^{+} ions in hCD2 are white and purple spheres, respectively; the corresponding metal ions in zCD2 are blue spheres. Only two active site residues differ between zCD2 and hCD2: N530 and N645 of zCD2 appear as D567 and M682 in hCD2, and these residues are located at the mouth of the active site, distant from the ligand binding site. **(c)** Molecular surface comparison of hCD2 (left) and zCD2 (right), color-coded by electrostatic potential (red to blue, -10 to 10 kT/e). TSA ligands are shown in ball-and-stick fashion to indicate the active site.

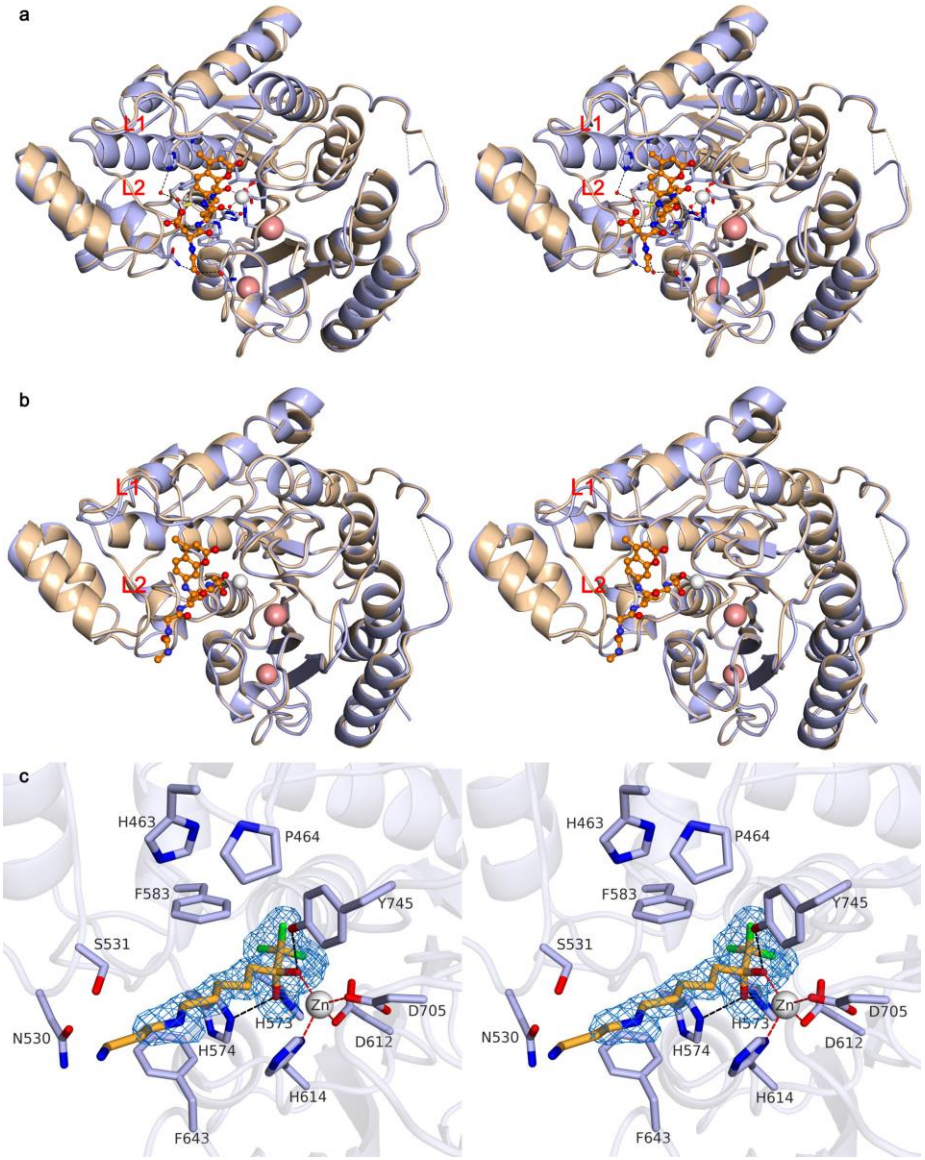

Supplementary Figure 6. Structure of zCD2. (a) Superposition of the zCD2-substrate **1** complex (light blue, dashed line indicating the disordered loop D770-H771) with unliganded zCD2 (wheat, dashed line indicating the disordered loop residues H771-L772). The substrate is indicated by a stick-figure; its N-terminal acetyl group and the serine side chain are not modeled due to disorder. The catalytic Zn^{2+} ion is a white sphere and two K^+ ions are salmon spheres. Only minimal structural changes accompany substrate binding. **(b)** Superposition of the zCD2-substrate **8** complex (light blue) with unliganded zCD2 (wheat, dashed line indicating the disordered loop residues H771-L772). The substrate is indicated by a stick figure; its N-terminal acetyl group and the arginine side chain are not modeled due to disorder. The catalytic Zn^{2+} ion is a white sphere and two K^+ ions are salmon spheres. Only minimal structural changes accompany substrate binding. **(c)** Simulated annealing omit map (blue mesh, 3.0σ) of the trifluoroketone inhibitor 7-[(3-aminopropyl)amino]-1,1,1-trifluoroheptan-2-one bound as a tetrahedral gem-diolate, which mimics the tetrahedral intermediate and its flanking transition states in catalysis (orange stick figure; F atoms are green); inhibitor O1 is closer to Zn^{2+} than O2, likely due to electrostatic stabilization of O1 as the oxyanion by Zn^{2+} coordination as well as the adjacent CF_3 group.

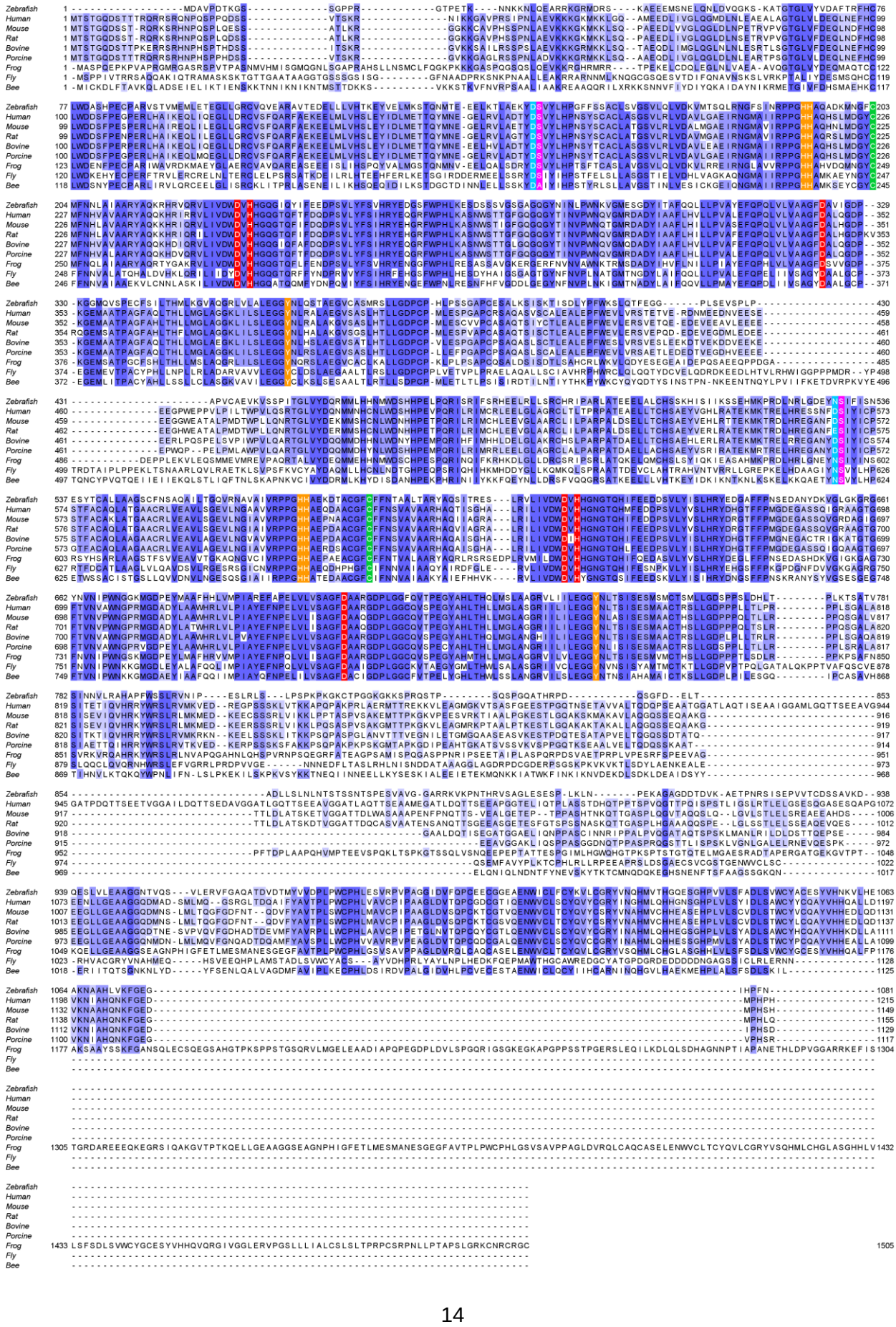
Zebrafish
Human
Mouse
Rat
Bovine
Porcine
Frog
Fly
Bee

Supplementary Figure 7. Sequence alignment of HDAC6 orthologues. In each domain, the Zn^{2+} ion binding residues are highlighted in red, the conserved catalytic residues in the active site are highlighted in orange, the aspartate residue interacting with the backbone NH groups flanking the acetyllysine substrate (D101 in HDAC8) is highlighted in sky blue, the newly identified conserved serine residue important for substrate binding in HDAC6 is highlighted in magenta, and the conserved buried active site cysteine residue is highlighted in green. Remaining conserved residues with are highlighted in blue. Sequence alignment prepared with Clustal Omega, figure prepared with Jalview.

.

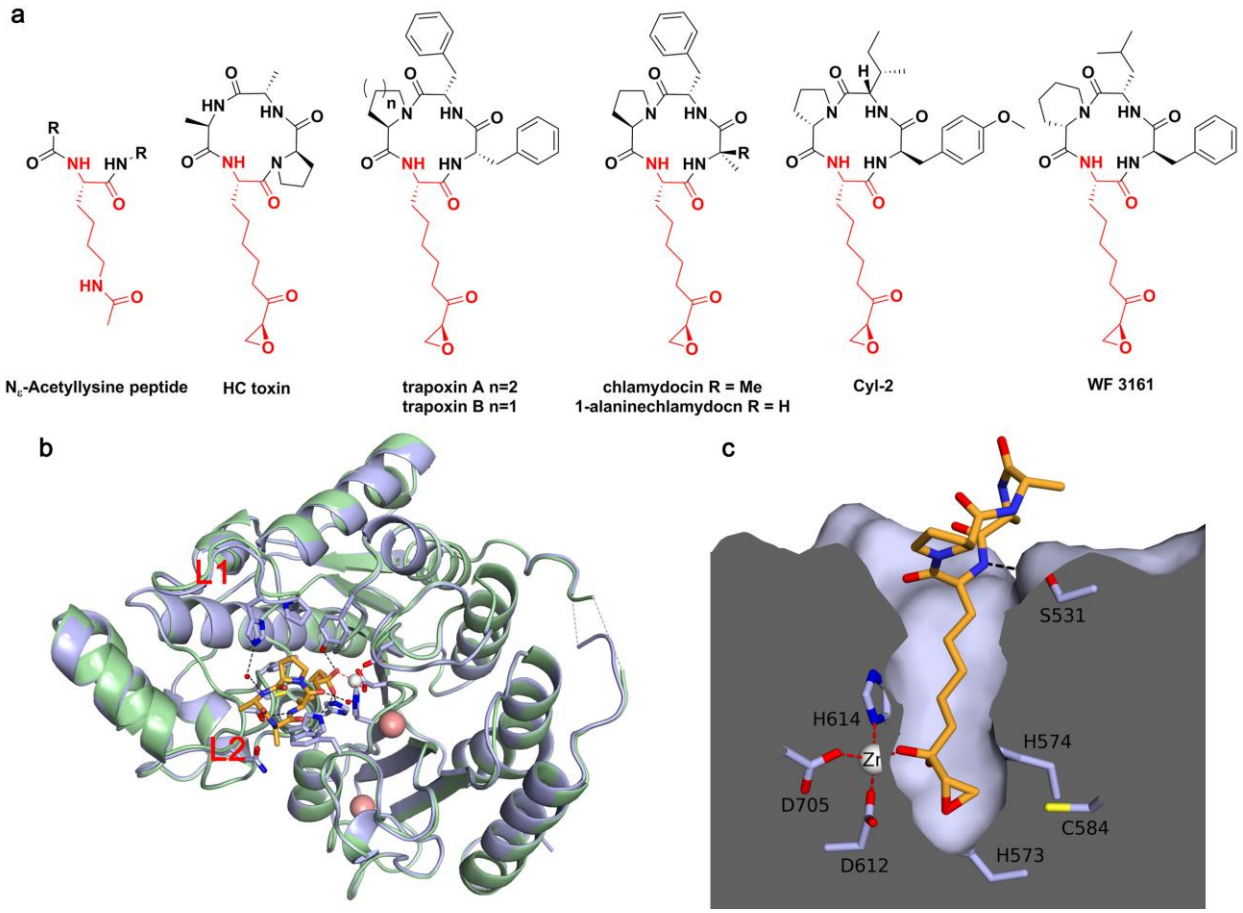

Supplementary Figure 8. Macrocyclic HDAC inhibitors, and structure of the zCD2-HC toxin complex. (a) A class of cyclic tetrapeptides containing 2-amino-8-oxo-9,10-epoxydecanoic acid (L-Aoe, red), which partially mimics the HDAC substrate Nε-acetyl-L-lysine. Both the terminal epoxide and adjacent carbonyl group of the Aoe side chain are essential for inhibitory potency against HDACs. **(b)** Superposition of the zCD2-HC toxin complex (light blue, white surface) with unliganded zCD2 (green) shows that the binding of HC toxin (orange stick figure) to zCD2 does not trigger any significant conformational changes. The Zn^{2+} ion, K^{+} ion, and water molecules are shown as white, salmon, and red spheres, respectively. Disordered segments are shown as dashed lines. Notably, this is the first crystal structure of HC toxin, and hence the first observation of the novel cis-trans-cis-trans peptide bond architecture of the cyclic tetrapeptide. **(c)** Close-up view of HC toxin binding, showing the solvent-accessible surface of the active site contour. Metal coordination and hydrogen bond interactions are shown in red and black dashed lines, respectively.

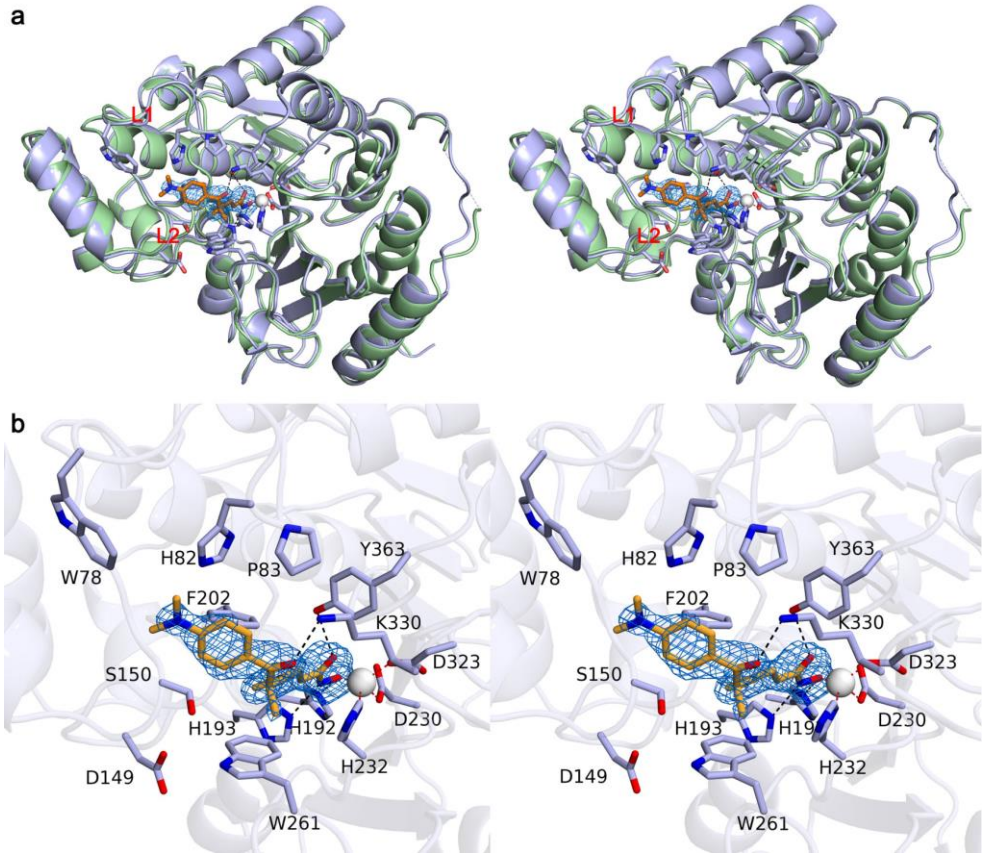

Supplementary Figure 9. Crystal structure of zCD1. (a) The overall structure of the zCD1-TSA complex (light blue) is highly similar to that of the zCD2-TSA complex (green), with an r.m.s. deviation of 0.58 Å for 311 Cα atoms. The simulated annealing omit map (blue mesh, 3.0σ) indicates TSA (orange) bound in the active site of zCD1; Zn^{2+} ions are shown as white spheres. **(b)** Close-up view of the zCD1 active site. Metal coordination and hydrogen bond interactions are shown as red and blue dashed lines, respectively.

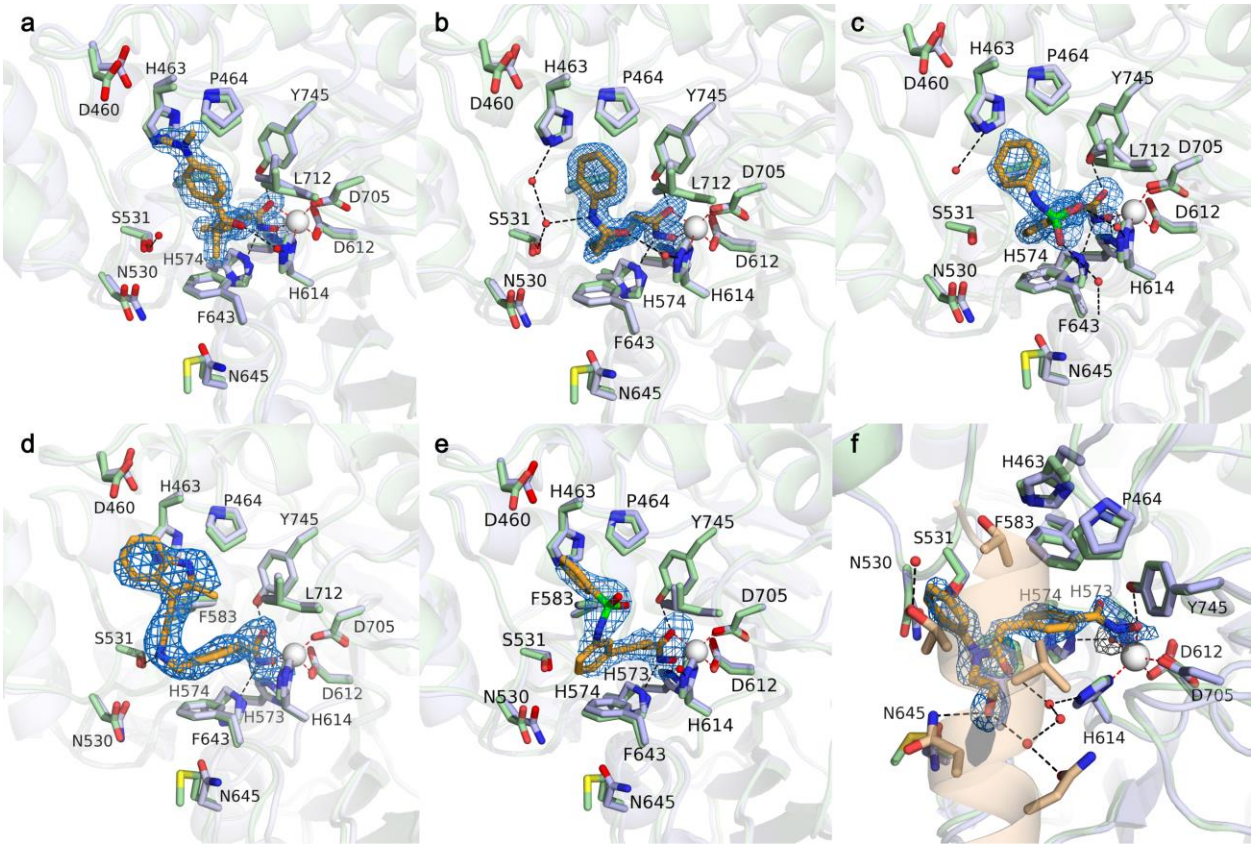

Supplementary Figure 10. Structures of zCD2 complexed with pan-HDAC inhibitors and HDAC6-specific inhibitor HPOB. Simulated annealing omit maps (blue mesh, 3.0σ) show each bound inhibitor. Metal coordination and hydrogen bond interactions are shown as red and black dashed lines, respectively; Zn^{2+} ions are shown as white spheres. Inhibitors are shown as ocher stick figures and are as follows: **(a)** TSA; **(b)** SAHA; **(c)** Belinostat; **(d)** Panobinostat; **(e)** Oxamflatin; and **(f)** HPOB. The cap region of HPOB interacts with an adjacent monomer (wheat helix) in the crystal lattice.

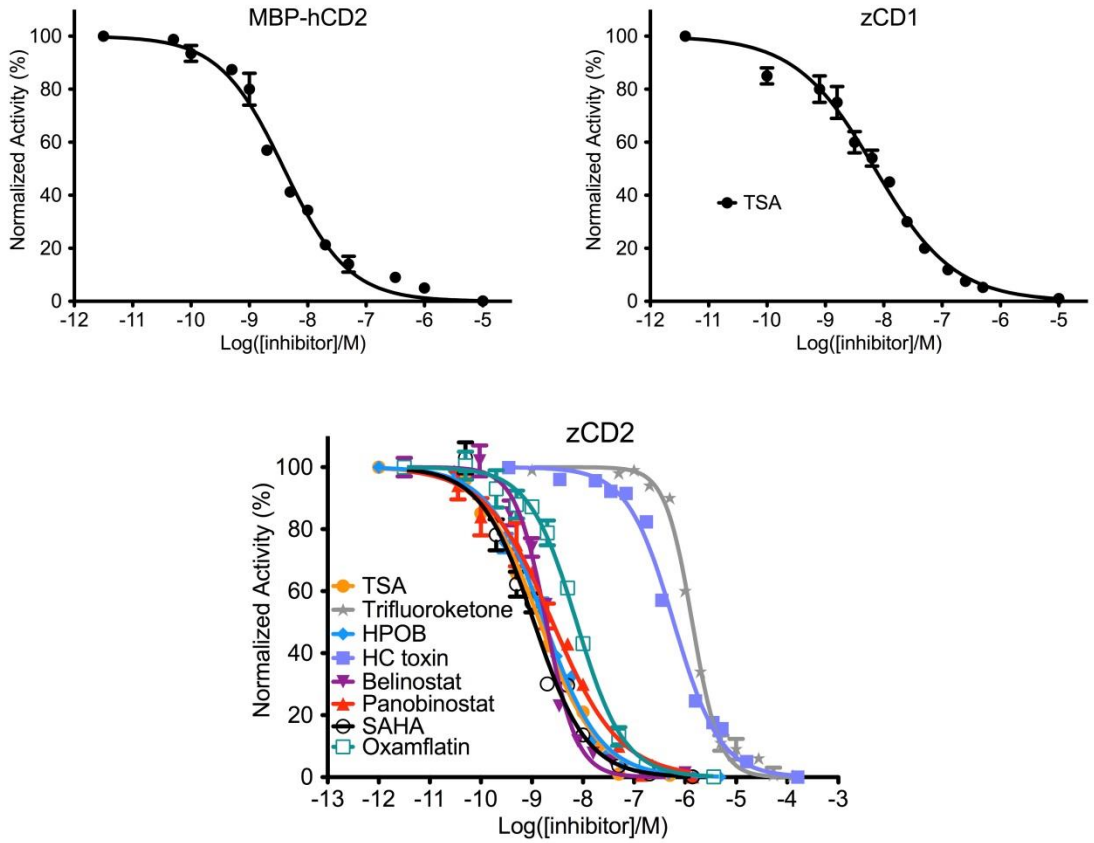

Enzyme	MBP-hCD2	zCD1	zCD2							
Inhibitor	TSA	TSA	TSA	HPOB	HC toxin	Trifluoro-ketone	Belinostat	Panobinostat	SAHA	Oxamflatin
IC_{50} (nM)	3.9 ± 0.8	7 ± 1	1.4 ± 0.2	1.8 ± 0.3	600 ± 90	1400 ± 200	1.9 ± 0.3	2.5 ± 0.5	1.1 ± 0.3	7.5 ± 0.9
K_i (nM)	2.2 ± 0.4	4.8 ± 0.7	0.8 ± 0.1	1.0 ± 0.2	350 ± 50	800 ± 100	1.1 ± 0.2	1.4 ± 0.3	0.6 ± 0.2	4.3 ± 0.5

Supplementary Figure 11. Inhibition of HDAC6 by inhibitors used in crystal structure determinations. Data were analyzed by logistic regression for IC_{50} determination and the inhibition constant K_i was calculated based on the Cheng-Prusoff equation assuming competitive inhibition, $K_i = IC_{50}/(1+[S]/K_M)$, as described in the Methods section. The enzyme concentrations used in this study were 3 nM for zCD2, 6 nM for MBP-hCD2, and 12 nM for zCD1. Since some IC_{50} values are near the measurement threshold of [enzyme]/2, these values should be regarded as upper limits since the actual IC_{50} may be even lower. Data represent mean ± s.e.m. (n=3).

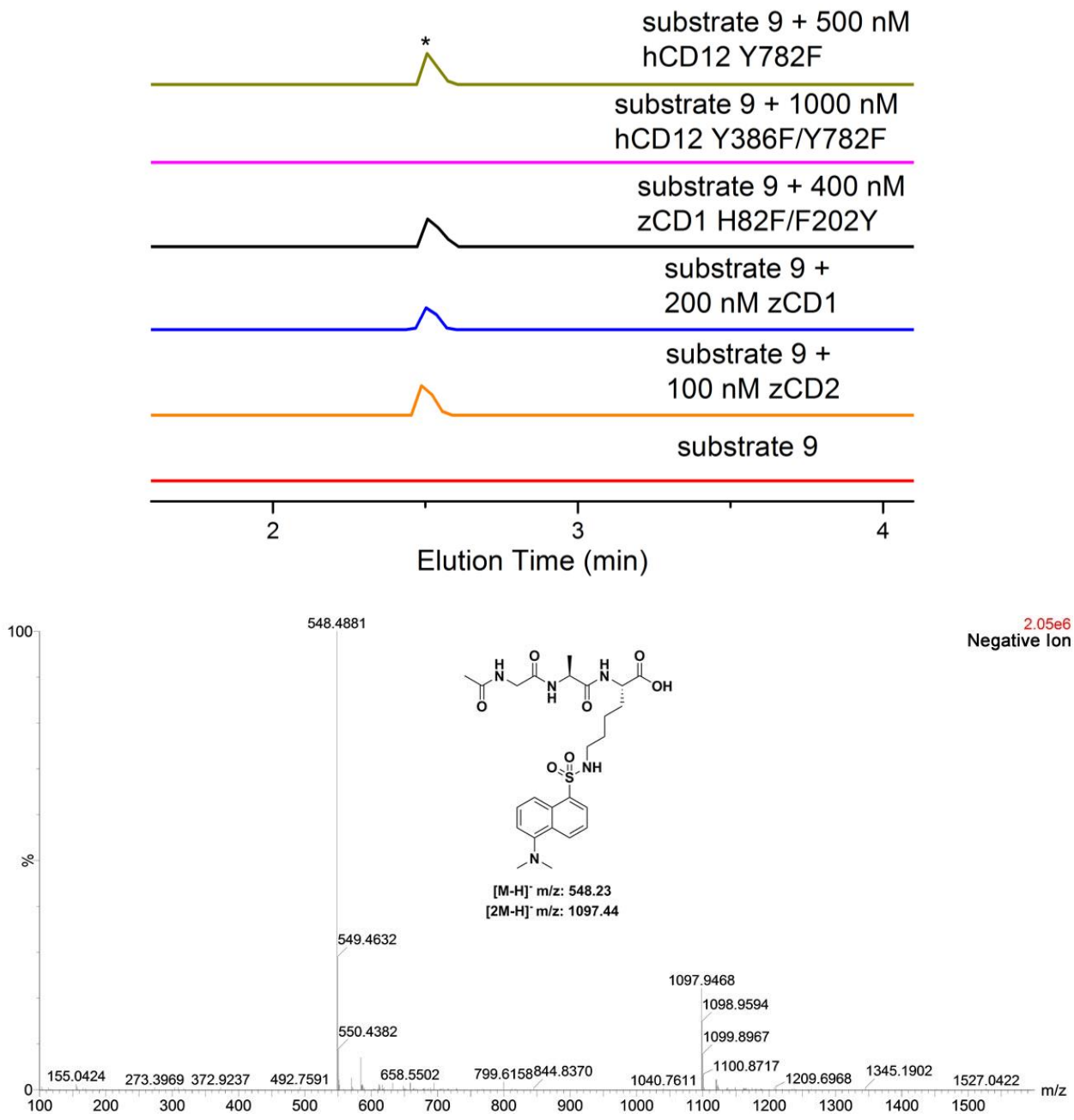

Supplementary Figure 12. Representative LC-MS traces (ESI-) of enzymatic reactions with substrate **9**. Due to its small size and polarity, the enzymatic product was dansylated in order to be efficiently separated from the reaction mixture for MS characterization. The enzymatic product can be quantified by comparing the integrated peak area with that of dansylamide (t_R = 2.40 min) as an internal standard to determine specific activity. The full mass spectrum of the dansyl-derivatized product peak (*) is shown below.

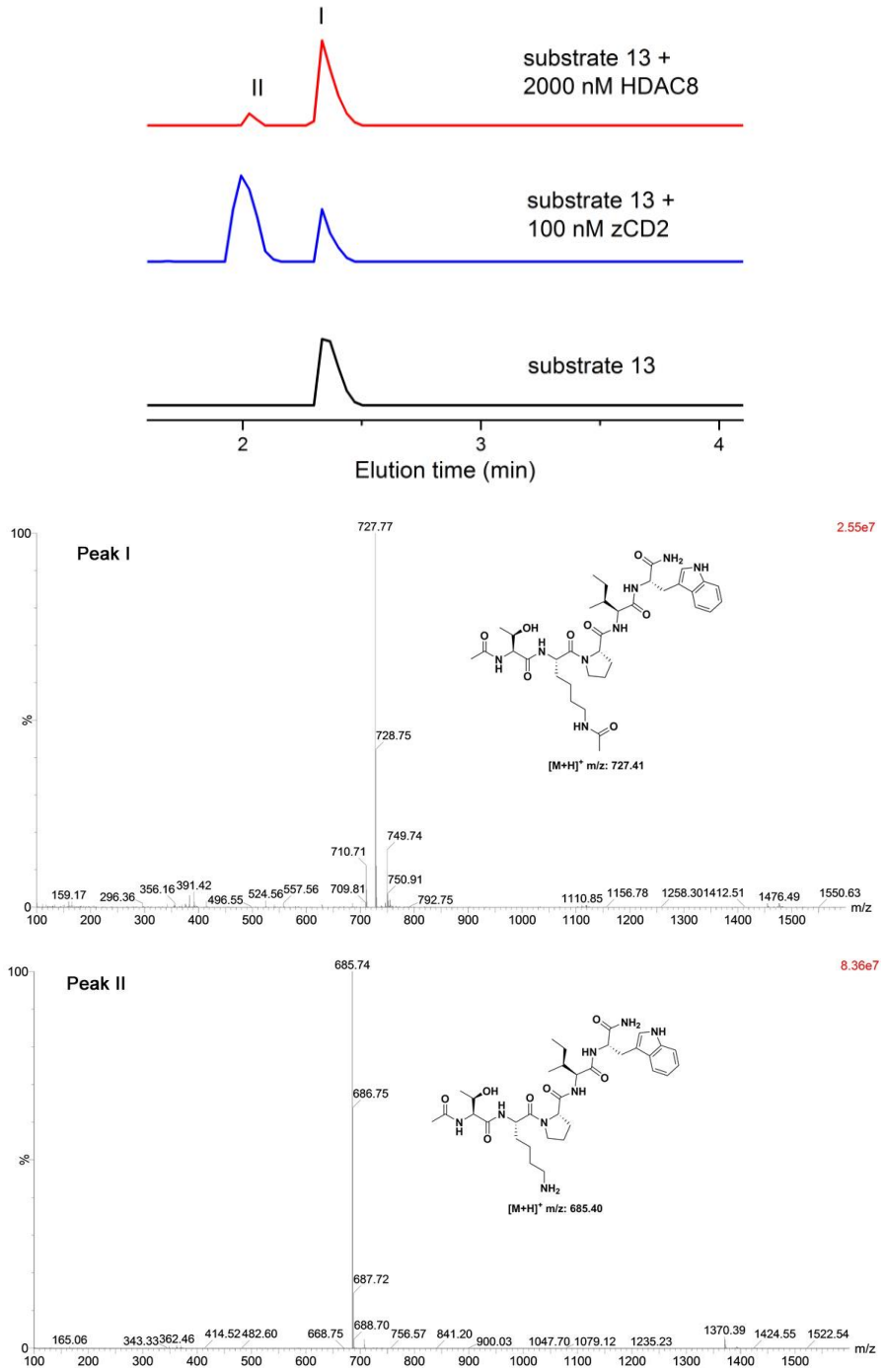

Supplementary Figure 13. Representative LC-MS traces (ESI+) of enzymatic reactions with substrate **13** (corresponding to residue T2930-W297 of Hsp90). Full mass spectra of substrate (I) and product (II) peaks are shown below. The enzymatic product can be quantified by comparing the integrated peak area with that of an authentic synthetic product peptide Ac-Thr-Lys-Pro-Ile-Trp-NH_2 as an external standard to determine specific activity.